Slow-Neutron Inelastic Scattering from Beryllium Powder*

R. E. SCHMUNK
Phillips Petroleum Company, Atomic Energy Division, Idaho Falls, Idaho
(Received 6 July 1964)

The inelastic scattering of slow neutrons by a sample of beryllium powder has been measured using the Materials Testing Reactor phased-chopper velocity selector. Data were obtained at incident neutron energies of 0.040, 0.0415, 0.070, and 0.10 eV and at room temperature for a sample which had a transmission of 87%. The data were converted to partial differential cross sections and to the scattering-law presentation $S(\kappa,\hbar\omega)$. In contrast to previous measurements, the scattering-law presentation of the data displays considerable structure which correlates directly with the interference condition for coherent scattering. Factors which contribute to the observed structure include the structure factor for neutron-phonon interactions and the phonon dispersion relation itself. Data from this experiment are compared with the dispersion relation for single-crystal beryllium and the calculated frequency distribution of beryllium.

I. INTRODUCTION

SLOW-NEUTRON inelastic-scattering measurements have generally centered in two specific areas: (1) coherent-scattering measurements from single crystals which yield the dispersion relations of these crystals, and (2) scattering from liquids, polycrystalline solids, and molecular systems of gases, many of which are incoherent scatterers.[1] In the latter group of experiments the results are often related to Van Hove's space-time correlation function $G(\mathbf{r},t)$.[2] It was felt that scattering measurements on beryllium powder should be made to supplement the previous measurements of the dispersion relations of single crystal beryllium,[3] and with this primary purpose in mind data have been obtained for a powder sample using the Materials Testing Reactor (MTR) phased-chopper velocity selector.[4] In addition, the results of this experiment are available for developing an understanding of the moderation process in reactors, and they provide a basis for comparison of data with the velocity selector experiment at Chalk River.[5]

Neutron scattering by an incoherent scatter obeys the energy- and momentum-conservation conditions, and the transfer of these quantities is given, respectively, by $\hbar\omega$ and $\hbar\boldsymbol{\kappa}$ where $\hbar$ is Planck's constant divided by 2π,

$$\Delta E = E - E_0 = \hbar\omega$$

and

$$\boldsymbol{\kappa} \equiv \mathbf{k}_0 - \mathbf{k}. \tag{1a}$$

The energy and wave vector of the incident and scattered neutrons are E_0, $\mathbf{k}_0$, and E, $\mathbf{k}$, respectively. In the case of a solid coherent scatterer, such as beryllium, the scattering process is further restricted by an interference condition and the wave-vector equation becomes[6]

$$\boldsymbol{\kappa} \equiv \mathbf{k}_0 - \mathbf{k} = 2\pi\boldsymbol{\tau} - \mathbf{q}, \tag{1b}$$

where $\boldsymbol{\tau}$ is a translation vector of the reciprocal lattice and $\mathbf{q}$ is the phonon wave vector. A knowledge of the crystal orientation, incident and final neutron energies, and the angle of scattering allow one to obtain a pair of numbers for ω and q in the scattering from a single crystal, and by varying the experimental parameters and observing many neutron-phonon interactions one is able to determine the dispersion relation $\omega(\mathbf{q})$ for the crystal. In the case of scattering from a polycrystal it is no longer possible to sort out pairs of ω and $\mathbf{q}$ values although the same restrictive conditions still apply in the scattering process.

A considerable portion of the theoretical scattering calculations that have been made have been done in the incoherent approximation.[7–10] Beryllium which is within 1% of being a completely coherent scatterer would appear to be a case where this approximation would be least applicable and the results of this experiment should serve as a good test case.

The scattering data in this experiment have been processed to partial differential cross sections $\sigma(E_0,E,\theta)$ and reduced partial differential cross sections or scattering law $S(\kappa,\hbar\omega)$[11,12] which are related through the

* Work performed under the auspices of the U. S. Atomic Energy Commission.

[1] A survey of recent work in the field together with references to earlier work may be found in *Proceedings of the Chalk River Symposium on Inelastic Scattering of Neutrons in Solids and Liquids* (International Atomic Energy Agency Vienna, 1963), Vols. 1 and 2.

[2] L. VanHove, Phys. Rev. **95**, 249 (1954).

[3] R. E. Schmunk, R. M. Brugger, P. D. Randolph, and K. A. Strong, Phys. Rev. **128**, 562 (1962).

[4] R. M. Brugger and J. E. Evans, Nucl. Instr. Methods **12**, 75 (1961).

[5] R. N. Sinclair, in *Proceedings of the Chalk River Symposium on Inelastic Scattering of Neutrons in Solids and Liquids* (International Atomic Energy Agency Vienna, 1963), Vol. 2, p. 199.

[6] B. N. Brockhouse and P. K. Iyengar, Phys. Rev. **111**, 747 (1958).

[7] D. E. Parks, General Atomic Report GA-2125, 1961 (unpublished).

[8] J. A. Young and J. U. Koppel, Nucl. Sci. Eng. **19**, 367 (1964).

[9] W. Marshall and R. N. Stuart, University of California Radiation Laboratory Report No. 5568, April 1959 (unpublished); also in Atomic Energy Commission Report TID-4500, 14th ed. (unpublished).

[10] L. S. Kothari and K. S. Singwi, J. Nucl. Energy **5**, 342 (1957).

[11] R. M. Brugger, Atomic Energy Commission Research and Development Report IDO-16694 (Rev.) July 1962 (unpublished). This report is also designated as Atomic Energy Commission Report TID-4500, 17th ed., TNCC-US-21 (Rev.) and EANDC-US-25 (unpublished).

[12] P. D. Randolph, Phys. Rev. **134**, A 1238 (1964).

equation

$$\sigma(E_0,E,\theta)=(E/E_0)^{1/2}\exp(-\hbar\omega/2k_BT)S(\kappa,\hbar\omega). \quad (2)$$

The constants T and k_B are the sample temperature in degrees Kelvin and Boltzmann's constant, respectively. Examples of the data are given in the form $\sigma(E_0,E,\theta)$ versus E and $\sigma(\lambda_0,\lambda,\theta)$ versus λ for several scattering angles θ, and the final presentation is made in the form $S(\kappa,\hbar\omega)$ versus $|\kappa|$ for constant values of the energy transfer $\hbar\omega$. The data of this experiment display a considerable amount of structure which were not reported in previous measurements on beryllium powder,[5] although the data from the two experiments agree in magnitude. The observed structure is shown to correlate directly with the interference condition of Eq. (1b) and the periodic nature of reciprocal space. The elastic portion of the scattering data are also presented in scattering law form $S(\kappa,\hbar\omega)$ and the observed structure in these data agrees well with the interference condition for Bragg scattering. Finally, the first moment of the energy transfer with respect to the scattering law has been evaluated for these data. At low values of momentum transfer the experimental first moment is high by a factor of 3 but comes into agreement with theory at higher values of momentum transfer. An approximate correction of the data for multiple scattering improves the agreement between experiment and theory for the first moment over the full range of momentum transfers observed.

II. EXPERIMENTAL ARRANGEMENT

Data for the powder beryllium experiment were obtained using the (MTR) phased-chopper velocity selector. The basic experimental facility has been described in detail elsewhere[4]; however, modifications of the facility are noted in the following paragraphs. More complete details of these and other velocity selector modifications will be published separately. In the course of a previous experiment[12] new 12-in.-diam rotating collimators were added to the rotor system with the result that the time-dependent background was reduced to a nearly constant level. With the background improvement additional scattering detectors were added to measure back-angle scattering as noted in Fig. 1.

Initial data were obtained at incident energies of 0.0415, 0.07, and 0.10 eV with the sample at room temperature for 14 scattering angles and a rotor speed of 6000 rpm. Because of structure which was observed in the scattering law presentation of the data,[13] additional runs were obtained with higher rotor speeds and with detector banks modified for improved angular resolution. With one exception all scattering angles were defined by a number of 1-in.-diam by 18-in. active length BF_3 detectors placed side by side and connected

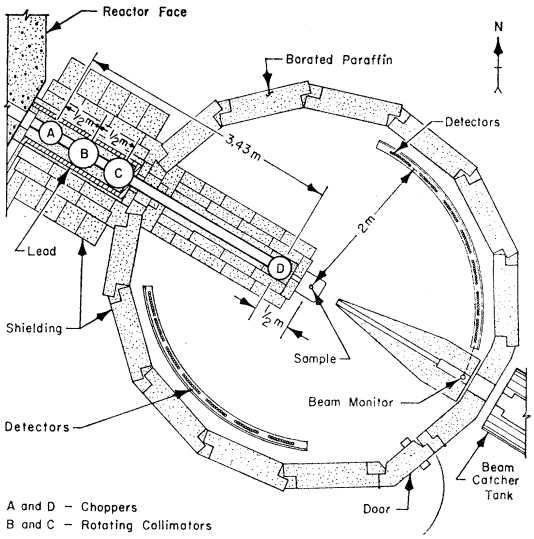

FIG. 1. Schematic drawing, plan view, of the MTR slow neutron velocity selector.

in parallel, and oriented with their center wires positioned vertically or normal to the scattering plane of the experiment. Angle 2 consisted of two groups of 1-in.-diam by 4-in. active length BF_3 detectors oriented in an element of solid angle above and below the horizontal plane. Initial measurements were made with all detector banks subtending an angle of 7.5° in the horizontal plane as measured from the sample position, while later measurements were made with 15 graduated detector banks, subtending 3.7° for the smallest scattering angle and increasing stepwise to 7.5° for the largest scattering angle.

Following the initial measurements which were made with a rotor speed of 6000 rpm, subsequent measurements were made with rotor speeds of 7500 rpm and 12 000 rpm. At 6000 and 7500 rpm the choppers and collimators were operated at the same speed, while at the higher chopper speed of 12 000 rpm the rotating collimators were spun at half-speed. The time resolution of the experiment $\Delta t/t$ as determined from the full width at half-maximum of the neutron burst at the beam monitor position was 4.2, 3.4, and 2.1% for chopper speeds of 6000, 7500, and 12 000 rpm, respectively, and an incident energy of 0.0415 eV.

The beryllium powder sample which had dimensions of 4.5 in.×4.5 in.×80 mil was held between 10-mil sheets of aluminum by clamps around the periphery of the sample with a spacer between the aluminum sheets to give the desired sample thickness. Filling of the sample holder was accomplished in a glove box which had positive air flow into the box at all times from leakage around access ports. Exhaust from the box passed through an absolute filter and vent scrubber system. The actual filling was done through a gap in the sample spacer at one corner of the holder. During the

[13] R. E. Schmunk, Bull. Am. Phys. Soc. 8, 322 (1963).

sample filling operation the sample holder was mounted in a vise block with the fill hole at the top, and the holder was agitated by placing it on a vibrator pad. It was desired to have a sample which would scatter 10% of the incident neutrons, but owing to the uncertainty of the powder density the final sample had a transmission calculated at 87.4% for the beryllium alone or 86.8% for sample and holder together when oriented at 45° to the incident beam. These values were obtained from the sample weight, area, and the average thickness which was determined from a mapping of the sample thickness. By comparison the observed sample transmission averaged over all data runs was 87.1%.

The sample material itself was QMV[13a] beryllium powder of approximately 100 mesh size. Principal contaminant of the sample was oxygen (0.473 wt.%) which, because of its scattering properties, was considered to have a negligible effect on the experimental results. Analysis of the sample for hydrogen indicated that it would contribute less than 1% to the scattering.

Forward scattering angles viewed the sample in transmission, and back scattering angles viewed the sample in reflection. Incident flux in the experiment was determined by a fission chamber which was placed in the forward beam, 2m from the sample. The sample and an identical empty sample holder were cycled into the beam at alternate 10-min intervals and running times for the different data runs ranged from 2000 to 4000 min for sample and empty holders individually. Detector pulses for the scattering detectors and beam monitor were stored in different sections of the 4096 channel time-of-flight analyzer. A channel width of 10 μsec and 256 channels per angle were used for all data runs.

A single data run was made at 0.10 eV with a thick sample (30% scatterer) to evaluate the effects of multiple scattering in the experiment. In addition to the measurements of inelastic scattering from beryllium, six additional runs of short duration were taken in order to study the elastic scattering. These latter measurements were made with the detector banks all reduced to an angular width of 3.7°.

III. TREATMENT OF EXPERIMENTAL DATA AND RESULTS

The general treatment of data in this experiment has followed the basic pattern of other MTR experiments,[14] with certain variations. After subtracting the empty-sample-holder data from the sample data, correcting for fast background, detector efficiency, incident flux, etc., the data were converted to partial-differential cross sections. Typical cross section profiles $\sigma(E_0,E,\theta)$ versus E are displayed in Fig. 2, and in Fig. 3 the same data are presented in the form $\sigma(\lambda_0,\lambda,\theta)$ versus λ. These

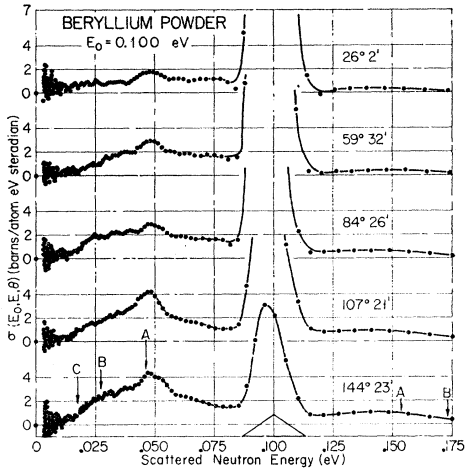

FIG. 2. Partial differential cross sections $\sigma(E_0,E,\theta)$ for scattering 0.100-eV neutrons from beryllium powder at room temperature. Points lettered A, B, and C relate the data to the frequency distribution of beryllium as discussed in the text.

data were obtained with a chopper speed of 6000 rpm and incident energy of 0.10 eV. In general the cross-section profiles are typified by an elastic peak superimposed on a low-intensity inelastic-scattering profile. The elastic peak in all cases matched closely the resolution width of the incident burst which was measured by the beam monitor. Also characteristic of the profiles are maxima which are present in the inelastic scattering at an energy change ΔE of approximately $2k_BT$ (0.05 eV). Errors due to counting statistics were evaluated channel by channel for all data; for the data of Figs. 2 and 3 these errors amount to about 5% at the peaks of the inelastic scattering, increasing as the cross section decreases. For the elastic portion of the spectrum the errors were generally less than 1%.

All of the data in this experiment were converted to scattering law, channel by channel, by inverting Eq. 2. The particular form of the scattering law used here is the reduced partial differential cross section[11] $S(\kappa,\hbar\omega)$. In the presentation of the data in scattering law form, $S(\kappa,\hbar\omega)$ is plotted as a function of $|\boldsymbol{\kappa}|$ for a constant absolute magnitude of the energy transfer $\hbar\omega$ which is referred to in terms of the dimensionless parameter $\epsilon=\hbar\omega/k_BT$. In the following discussion we shall use κ in referring to $|\boldsymbol{\kappa}|$.

The scattering law has been evaluated for specific values of the parameter ϵ for each scattering angle by an interpolation procedure which fits a parabola to four data points, two on each side of the energy of interest. A statistical error was obtained for each point of interpolated $S(\kappa,\hbar\omega)$, hereafter referred to as S_{int}, by taking one-half the sum of the absolute values of the errors ΔS for the two nearest data channels in the interpolation process, one on either side of the position in the energy spectrum which corresponds to the desired value of ϵ. Plots of the data in scattering law form serve as an

[13a] A Brush Beryllium Corporation Trademark.

[14] P. D. Randolph, R. M. Brugger, K. A. Strong, and R. E. Schmunk, Phys. Rev. 124, 460 (1961).

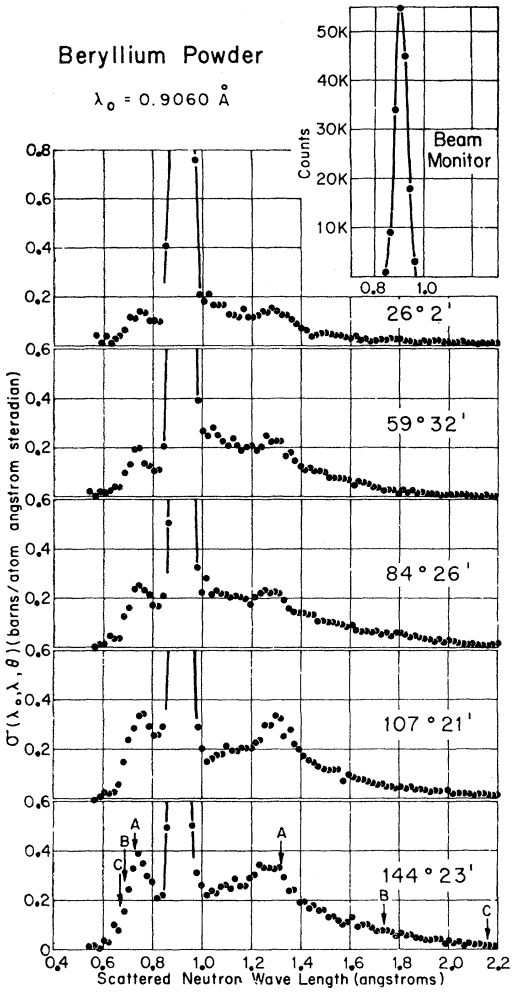

FIG. 3. Partial differential cross sections $\sigma(\lambda_0,\lambda,\theta)$ for scattering 0.100-eV neutrons from beryllium powder at room temperature. Points lettered A, B, and C relate the data to the frequency distribution of beryllium as discussed in the text.

internal check on the data since $S(\kappa,\hbar\omega)$ obeys the condition of detailed balance and is even in the magnitude of the momentum transfer and in the energy transfer $\hbar\omega$ and, therefore, points for positive and negative $\hbar\omega$ should plot together. This presentation also permits a direct comparison of data taken at different incident energies and reveals errors such as incorrect flux normalization. With 15 scattering angles, one obtains a maximum of 30 points on a plot of S_{int} for a given ϵ, provided both energy gain and loss events can be observed for the particular incident energy E_0. Combining data from different runs, a plot of S_{int} versus κ may contain as many as several hundred points for a particular value of ϵ. A typical example of such data is given in Fig. 4 for $\epsilon=1.75$ where a total of 183 points were plotted.

It should be noted that up to this point the data have not been averaged, and the only deviation from a channel-by-channel treatment of the data was in the interpolation procedure which was used to obtain S_{int}. Because the scattering law $S(\kappa,\hbar\omega)$ is overdetermined by the large number of data points, the data for S_{int} have been averaged and are presented in composite form in Fig. 5. The overdetermination of the data is due to the overlapping of the data which were obtained at different incident energies. This is demonstrated in the data of Fig. 6. In averaging the data, the range of κ values which was covered for a given ϵ was divided into a number of equal increments in $\ln\kappa$, and all data points which fell within the given increment were averaged together. For the set of data points which fell in a given increment in κ the arithmetic mean of κ was determined from the κ values on the individual points, and a weighted average for S was obtained for the scattering law from the individual S_{int} values. The weights assigned in the averaging process were determined from the statistical errors assigned to each S_{int} point, and the average $\bar{S}$ was determined according to the following equation:

$$\bar{S}=\sum_{i=1}^{N}\frac{S_i}{\delta S_i^2}\Big/\sum_{i=1}^{N}\frac{1}{\delta S_i^2} \tag{3}$$

The symbol S_i refers to the individual values of S_{int}, and δS_i is the statistical error of S_i. The number of data points which fall in the given increment in $\ln\kappa$ is N.

In addition, errors were computed for each of the averaged points according to two different formulas as follows:

$$\delta\bar{S}=\left[\sum_{i=1}^{N}\frac{(S_i-\bar{S})^2}{\delta S_i^2}\Big/N\sum_{i=1}^{N}\left(\frac{1}{\delta S_i}\right)^2\right]^{1/2} \tag{4}$$

and

$$\delta\bar{S}=\left[\sum_{i=1}^{N}(1/\delta S_i)^2\right]^{-1/2}. \tag{5}$$

The first of these formulas, Eq. (4), measures the standard deviation of the individual points S_i from the mean value $\bar{S}$, and the second, Eq. (5), gives a measure of the

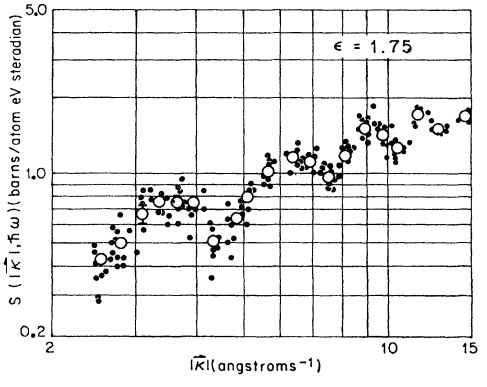

FIG. 4. Beryllium reduced partial differential cross sections from the individual data runs (solid points) compared with the same data after averaging (open points). Note the overdetermination of the data from the individual runs.

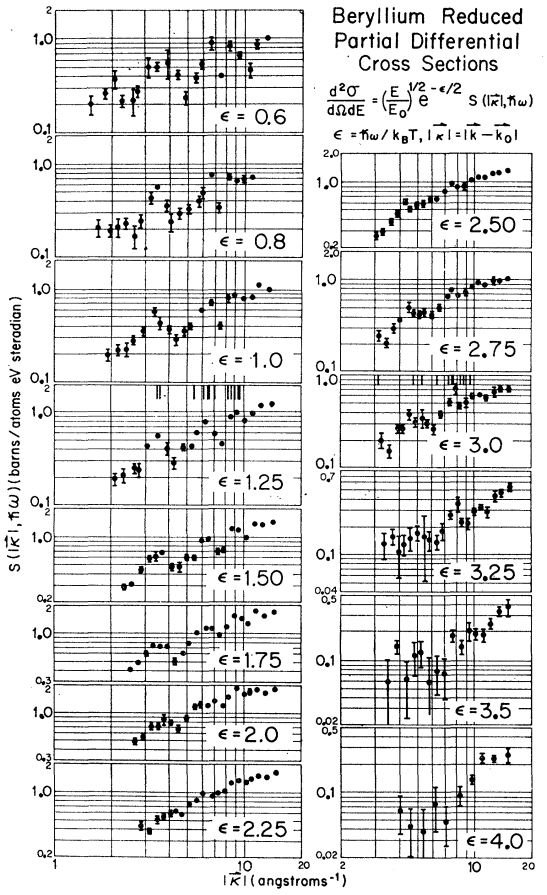

FIG. 5. A composite of the reduced partial differential cross sections for room-temperature beryllium powder. The data have been averaged and errors evaluated as discussed in the text. Errors, where bars are not displayed, are smaller than the size of the points.

statistical error on the mean value. To put it another way, Eq. (4) indicates the spread in the individual scattering law values which are averaged together, and Eq. (5) is a measure of the over-all counting statistics for the averaged point. In the presentation of the averaged data the larger of the two errors has been displayed, and the point is made here that there were no consistent differences between the errors evaluated by the two formulas. Where no error bars are displayed the errors on the averaged points are smaller than the plotting symbols. The number of increments which were chosen in averaging the data was arbitrary and was selected to match approximately the angular resolution of the experiment. Referring again to Fig. 4 the averaged data points are displayed together with the individual S_{int} points for comparison. The data handling which has been described here was done entirely by computer, and only where it could be established that the data were inconsistent for some valid physical reason were any of the data rejected.

Treatment of the Bragg data differed from that for the inelastic data. From an inspection of the cross section profiles of Figs. 2 and 3, it is possible to separate out the elastic portion of the scattering because the strong peaks centered at E_0 approximate closely the width of the beam monitor peak which is measured for a flight path equal to that for the scattering detectors. Although the elastic peaks varied in magnitude, they were observed in all scattering angles, even for scattering angles which did not satisfy the Bragg condition. The total count in each elastic peak was summed over the number of time channels equivalent to the monitor peak width and this number converted to scattering law. All elastic-scattering data have been treated in this way and are presented in Fig. 6. These data were all obtained with detector banks reduced in area with the exception of several data points for incident energies of 0.07 and 0.10 eV which appear at high values of κ, a region not covered by the other data.

IV. DISCUSSION

From the cross-section profiles of Figs. 2 and 3 it is evident that the separation of the scattering into elastic and inelastic contributions is straightforward. In the case of Bragg scattering from a crystal the interference condition of Eq. (1b) becomes $\mathbf{k}_0 - \mathbf{k} = 2\pi\boldsymbol{\tau}$. This implies that first-order Bragg scattering from a given set of planes in the crystal will contribute to the scattering law of Fig. 6 at a single value of $|\boldsymbol{\kappa}| = 2\pi/d_{hkl}$ where d_{hkl} is the spacing between crystalline planes of the set (hkl). Vertical slash marks above the κ scale of Fig. 6 indicate at what values of κ the various planes contribute to the scattering, and these values are listed in

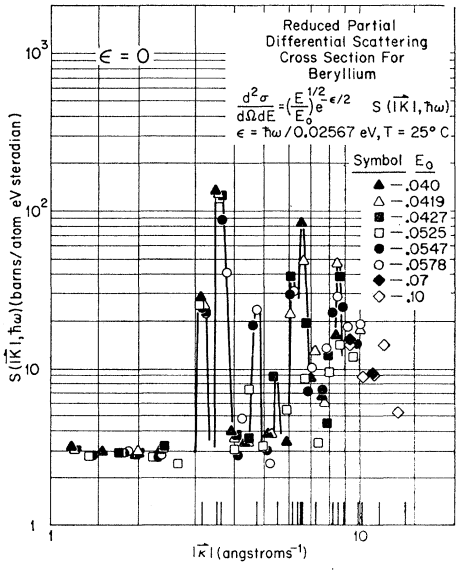

FIG. 6. Reduced partial differential cross sections for elastic scattering from beryllium powder at room temperature. The slash marks above the $|\boldsymbol{\kappa}|$ scale indicate values of $|\boldsymbol{\kappa}|$ at which the different crystalline planes contribute to the Bragg scattering from the solid.

TABLE I. A partial listing of κ values for which Bragg scattering from the planes (hkl) contributes to the scattering law $S(\kappa,\hbar\omega)$.

(hkl)	$\lvert\boldsymbol{\kappa}\rvert = 2\pi/d_{hkl}$	(hkl)	$\lvert\boldsymbol{\kappa}\rvert = 2\pi/d_{hkl}$
(010)	3.174 Å^{-1}	(022)	7.253 Å^{-1}
(002)	3.507 Å^{-1}	(023)	8.245 Å^{-1}
(101)	3.627 Å^{-1}	(120)	8.398 Å^{-1}
(012)	4.730 Å^{-1}	(121)	8.580 Å^{-1}
(110)	5.498 Å^{-1}	(114)	8.912 Å^{-1}
(013)	6.144 Å^{-1}	(122)	9.101 Å^{-1}
(020)	6.349 Å^{-1}	(302)	10.148 Å^{-1}
(112)	6.521 Å^{-1}	(222)	11.541 Å^{-1}
(021)	6.587 Å^{-1}	(321)	13.947 Å^{-1}

Table I. Magnitudes of the peaks in the structure are sensitive to energy and angular resolutions as these peaks should properly be delta functions. Single Bragg scattering cannot occur for $\kappa < 3.174$ Å^{-1}, and data for lower κ values correspond to incoherent and multiple Bragg scattering effects. Measurement of the incoherent contribution[15] to the elastic scattering places an upper limit of 0.23 b/atom-eV-sr to the data at low κ values in Fig. 6. Hence, for all practical purposes the data at low κ represent multiple Bragg scattering. Vineyard[16] has evaluated multiple scattering from a plane slab for several cases, and although none of these cases correspond exactly to the present situation they indicate that the observed scattering (13% compared to a predicted 20%) is of the correct magnitude. The fact that no structure is observed in the multiple scattering is not surprising. The primary Bragg scattering from a given set of crystalline planes in the sample is confined to a conical element of solid angle, $2\pi \sin\theta_B d\theta$, or diffraction halo symmetric about the direction of the incident beam where the scattering angle θ is twice the Bragg angle θ_B. All directions which are included in this element of solid angle must necessarily be considered as directions of incidence for a second scattering process. Then neutrons which are double Bragg scattered are distributed in observed scattering angles between 0 and $4\theta_B$. From the above considerations higher order contributions to the multiple scattering would not be expected to produce structure in the observed data either.

In the averaging of the inelastic scattering data for values of $\epsilon = \hbar\omega/k_B T$ less than 1.5, only data points corresponding to energy gain were averaged because of a splitting which existed between the energy gain and loss data, in violation of the detail balance condition. The splitting was determined experimentally to be due to air scattering of the primary scattered neutrons, which had the effect of increasing the neutron flight path such that the air scattering contributed only to the energy-loss portion of the spectrum. Effects of air scattering were studied with a vanadium sample which gave a scattering spectrum[17] similar to that from beryllium, i.e., a strong elastic-scattering peak with low-intensity inelastic wings on both energy gain and loss sides of the peak. It was found that by using a helium atmosphere flight path over the distance from D rotor to the sample and from the sample to a given detector, with cadmium collimation along the flight path, that the scattering law data for energy losses were reduced in magnitude to the point where they agreed with the energy gain data. For $\epsilon \geq 1.5$ the energy gain and loss data agreed and both were included in the averaging. For averaging, the κ scale was divided into 20 equal increments in ln κ, except for the highest values of ϵ where the number of increments was reduced. In the averaged data of Fig. 5 for $\epsilon \geq 1.5$ each data plot represents a 9:1 reduction in the number of data points from the S_{int} data and for $\epsilon < 1.5$ the reduction is about 6:1. Scattering law values were not obtained for $\epsilon < 0.6$ because of the nearness to the elastic peaks in the scattering profiles.

The averaged data clearly display the structure which was observed in the initial data. It should be noted that the magnitude of the scattering law increases with increasing ϵ up to $\epsilon = 2.0$ ($\hbar\omega = 0.0513$ eV) and then decreases in magnitude, particularly for $\epsilon > 3.0$. The maximum in the scattering law at $\epsilon = 2.0$ agrees well with a peak in the frequency distribution which occurs at $\omega = 8\times10^{13}$ sec^{-1}.[8,18] In Figs. 2 and 3 the energies and wave lengths at points labeled A, B, and C correspond to the two peaks in the frequency distribution of beryllium and the maximum frequency in the distribution, respectively. The scattering law data for $\epsilon > 3.25$ are due to multiphonon processes as these energy changes correspond to frequencies which are greater than the maximum optical frequency of the beryllium dispersion relation.[3]

These results are in marked contrast to the data of Sinclair[5] which do not show any structure in the usual presentation (S versus $\lvert\boldsymbol{\kappa}\rvert$ for constant $\hbar\omega$), although the data from the two experiments agree approximately in magnitude.[11] It is interesting that Sinclair attributed the failure to observe structure in the scattering law as due to poor angular resolution which was better than the angular resolution of the first phases of this experiment. The difference in the results of the two experiments may be due in part to a thicker sample (transmission of 0.817) which was used for some of Sinclair's measurements.

The structure in the present scattering law data is considered to be real and is discussed further in the following. A close examination of the data of Fig. 5 reveals that maxima which are observed in the scattering-law data for $\epsilon \leq 2$ tend to fall at the same values of κ for different values of ϵ, and the structure which

[15] D. J. Hughes and R. B. Schwartz, Brookhaven National Laboratory Report No., BNL-325, 2nd ed., Superintendent of Documents, U. S. Government Printing Office, Washington, D. C., 1958 (unpublished).

[16] G. H. Vineyard, Phys. Rev. **96**, 93 (1954).

[17] R. M. Brugger (private communication).

[18] J. A. Young, Bull. Am. Phys. Soc. **9**, 414 (1964).

appears for $\epsilon \geq 2.75$ has maxima at κ values which correspond to minima for $\epsilon \leq 2$. Comparing the present data with the dispersion relations for beryllium[3] indicates that the structure observed in Fig. 5 for $\epsilon \geq 2.75$ is in the frequency region where neutrons can interact only with the optical vibrations of the solid and for $\epsilon \leq 2.0$ the interactions are primarily with the acoustical vibrations. Inelastic scattering from the powder sample is governed by the same conditions as the scattering from single-crystal beryllium which include the conservation conditions expressed in Eq. (1) and the structure factor[6] $g_j^2(\mathbf{q})$ which itself includes the polarization factor $(\boldsymbol{\kappa}\cdot\boldsymbol{\xi})^2$. Scattering at a given angle in the single-crystal experiment revealed a number of coherent peaks in the time distribution of the data, each peak corresponding to the neutron interaction with phonons of some particular frequency and wave vector, whereas the scattering from the powder gives a less distinctive continuous distribution which is actually a superposition of the scattering from many small crystals. A cut through the data of Fig. 5 at a constant value of κ defines a sphere of radius κ in wave vector space, and the data at a given value of κ include all neutron-phonon interactions whose wave vector plots terminate on the surface of the sphere. In the data of Fig. 5 these interactions are classified according to the energy exchange in the interaction as specified by the parameter $\epsilon=\hbar\omega/k_BT$.

To relate the present data more closely to the single-crystal experiment the structure factor g_j^2 indicates in what regions of reciprocal space the neutron-phonon cross section is highest for a given type of lattice vibration. In regions of k space where the structure factor for beryllium is near its maximum value for one of the acoustical branches it is near maximum for the other acoustical branches as well and near a minimum for the optical branches. Conversely where the structure factor is near a maximum for the optical branches it is near a minimum for the acoustical branches. The regions of k space referred to here are the Brillouin zones of the extended zone scheme, and scattering from a given zone is restricted to a certain range of κ values. This restriction is particularly severe for the low acoustical frequencies which correspond to the region near the origin of the dispersion relation. For these low frequencies κ is restricted to a small region $2\pi|\boldsymbol{\tau}|-|\mathbf{q}| \leq |\boldsymbol{\kappa}| \leq 2\pi|\boldsymbol{\tau}|+|\mathbf{q}|$ near the center of the Brillouin zone.[19] For the higher acoustical frequencies the restriction becomes less severe. A clear picture of the restrictions could be obtained from a mapping of the frequency contours throughout the full Brillouin zone. Basically then there are two restrictions which affect the structure in the scattering law: (1) the structure factor which limits interactions with each branch of the dispersion relation to particular zones of the extended zone scheme and (2) the relation between phonon frequency ω and wave vector $\mathbf{q}$ which limits interactions with low acoustical frequencies even further. One would expect the structure effects to be sharpest at low values of ϵ which agrees well with the data of Fig. 5. In fact, in the limit as one considers lower and lower values of ϵ the observed structure should compare more closely with the elastic-scattering data of Fig. 6. On the other hand, the optical branches, which span a narrower band of frequencies, contribute to the scattering over a larger portion of the Brillouin zone for the appropriate ϵ indicating that the structure which is observed at the higher frequencies would not be as sharp as for the low-energy acoustical transitions. In the range $2.25 \leq \epsilon \leq 2.5$ there is considerable overlapping of the acoustical and optical branches of the dispersion relation which would appear to negate the dominance of the structure factor.

We can obtain an average value of κ for the scattering from a given zone by considering a vector drawn from the origin to the lattice point at the center of that zone. In Table II are listed the values for the magnitudes of wave vectors joining the origin of wave vector space with a particular lattice point (hkl) together with the multiplicity factor n for the given point. The values of Table II are sorted according to whether the structure factor is higher for optical or acoustical transitions in the given zone. Because of the periodic nature of wave vector space and the properties of the structure factor which were noted previously, the scattering cross section and scattering law are not monotonically increasing functions of κ but rather will fluctuate depending on the number of Brillouin zones which contribute to the scattering for a given range of κ values. Comparison of the κ values of Table II with the scattering law data of Fig. 5 indicates a definite correlation between the two. To aid in making the comparison, slash marks have been added above the data plots for $\epsilon=1.25$ and $\epsilon=3.0$

TABLE II. A partial listing of κ values for wave vectors drawn from the origin to the center of the (hkl) Brillouin zones of multiplicity n. The listing is separated according to zones in which neutron-phonon interactions are predominant for either acoustical or optical frequencies as predicted by the structure factor.

Acoustial			Optical		
(hkl)	n	$\lvert\boldsymbol{\kappa}\rvert=2\pi\lvert\boldsymbol{\tau}\rvert$	(hkl)	n	$\lvert\boldsymbol{\kappa}\rvert=2\pi\lvert\boldsymbol{\tau}\rvert$
(002)	2	3.507 Å^{-1}	(001)	2	1.754 Å^{-1}
(011)	12	3.627 Å^{-1}	(010)	6	3.174 Å^{-1}
(110)	6	5.498 Å^{-1}	(012)	12	4.730 Å^{-1}
(013)	12	6.144 Å^{-1}	(003)	2	5.261 Å^{-1}
(112)	12	6.521 Å^{-1}	(020)	6	6.349 Å^{-1}
(021)	12	6.587 Å^{-1}	(022)	12	7.253 Å^{-1}
(004)	2	7.014 Å^{-1}	(113)	12	7.609 Å^{-1}
(023)	12	8.245 Å^{-1}	(014)	12	7.699 Å^{-1}
(121)	24	8.580 Å^{-1}	(120)	12	8.398 Å^{-1}
(114)	12	8.912 Å^{-1}	(005)	2	8.767 Å^{-1}
(015)	12	9.324 Å^{-1}	(122)	24	9.101 Å^{-1}
(030)	6	9.523 Å^{-1}	(024)	12	10.03 Å^{-1}

[19] P. A. Egelstaff, in *Proceedings of the Chalk River Symposium on Inelastic Scattering of Neutrons in Solids and Liquids* (International Atomic Energy Agency, Vienna 1963), Vol. 1, p. 65.

at κ values given in Table II for acoustical and optical transitions, respectively. Consideration has not been given to the polarization factor $(\boldsymbol{\kappa}\cdot\boldsymbol{\xi})^2$ which plays an important part in determining the cross section for a given interaction; however, no distinction has been made between longitudinal and transverse modes of vibration either. The preceding explanation of the structure in the inelastic-scattering data is supported by preliminary scattering law data for aluminum powder[20] and could be tested further for beryllium by taking additional data at high-energy transfers ($\epsilon\approx 3.0$) and low-momentum transfer (low κ). According to the information in Table II further structure should appear in the scattering law near κ values of 3.17 Å^{-1} and 1.75 Å^{-1} for high-energy transfers.

Egelstaff[21] has used an extrapolation technique to derive from scattering law data what he calls a generalized frequency distribution. In the extrapolation process it is necessary to use scattering law data from an intermediate range of κ values such that structure effects from interference scattering, which are important at low κ, are damped out and yet contributions from multiphonon scattering, which are important at large κ, are not contributing. The data from this experiment indicate that at least in the case of beryllium this extrapolation would be difficult to make because the structure is observed over nearly the full κ range of the scattering law data.

The first moment of the energy transfer with respect to the scattering law has been evaluated for the data of this experiment from the following equation

$$\langle\epsilon'\rangle = A\int_0^\infty \epsilon \sinh(\epsilon/2)S(\kappa,\hbar\omega)d\epsilon = \hbar^2\kappa^2/2Mk_BT.$$

The constant $A=8\pi k_BT/\sigma_b$ where σ_b is the bound atom scattering cross section of beryllium and M is the mass of the beryllium atom. Evaluation of the integral is made at constant κ or momentum transfer. Values were taken from the data of Fig. 5 at particular values of κ, and the integration was done by planimeter, terminating the integral at an upper limit of $\epsilon=4.5$.

In Fig. 7 the results of this evaluation are displayed as the ratio of experimental to theoretical first moment as a function of κ. The experimental first moment shows a strong κ dependence, being high by as much as a factor of 3 at small κ and low for larger κ. Errors in the scattering law data which were used in this analysis are less than $\pm 15\%$ for all but the highest energy transfers and less than $\pm 5\%$ for the data in the region near $\epsilon=2.0$. The fact that the experimental first moment is low at high κ is not serious since this indicates that the integration has not been extended to high enough

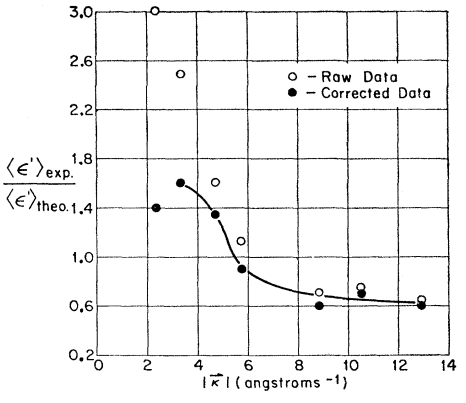

FIG. 7. Ratio of the experimental to theoretical first moment of the energy transfer with respect to the scattering law as a function of $|\boldsymbol{\kappa}|$ (proportional to momentum transfer). The solid points were obtained after applying a multiple scattering correction to the scattering law data.

energy transfers where the scattering is due entirely to multiphonon processes. The approximate $1/\kappa^2$ dependence of the first moment at low κ suggests that multiple scattering is contributing to the data,[12] although with a sample which gave a total scattering of 13% the contributions from multiple scattering should be small. From the analysis of the elastic scattering data, in which a contribution of 13% from multiple scattering was observed, one might estimate a contribution to the inelastic data from multiple scattering of about the same magnitude. The most important contribution to the inelastic-scattering data from multiple scattering should be from phonon-Bragg and Bragg-phonon double scattering and should amount to about 13%. The reasoning applied here is related to the neutron mean free path which is smallest for Bragg scattering. Hence, either preceding or following an inelastic-scattering event there is the probability of Bragg scattering which is much higher than the probability for a second neutron-phonon interaction. Contributions from phonon-phonon double scattering and higher order events should amount to about 1%. Following the work of Sakamoto[22] and of Randolph[12] a quantitative estimate of the multiple scattering has been obtained by fitting a polynomial to the scattering law data

$$S(\kappa,\hbar\omega)=A_0(\epsilon)+A_1(\epsilon)\kappa^2+A_2(\epsilon)\kappa^4+\cdots.$$

Since theoretical expressions for the scattering law start with the second-order term, the $A_0(\epsilon)$ term is assumed to give the contribution from multiple scattering. The assumption of an isotropic contribution from multiple scattering is in agreement with the data obtained with a 30% scatterer, which are generally higher in magnitude over the full range of momentum transfers observed. A polynomial fitting was made to

[20] Data obtained by P. D. Randolph and R. M. Brugger of this laboratory.

[21] P. A. Egelstaff, in *Proceedings of the Symposium on Inelastic Scattering of Neutrons in Solids and Liquids*, (International Atomic Energy Agency Vienna, 1961), p. 25.

[22] M. Sakamoto, B. N. Brockhouse, R. G. Johnson, and N. K. Pope, J. Phys. Soc. Japan, Suppl. **BII**, 370 (1962).

the data of Fig. 5 for each value of the energy transfer, ignoring the extrema in the structure. The zero-order terms were then used to correct the scattering law data and re-evaluate the first moment $\langle\epsilon^1\rangle$ which is displayed in Fig. 7. The corrected first moment agrees much better with theory; however, the procedure used in correcting the data is open to question considering the fact that beryllium is a coherent scatterer.

V. CONCLUSIONS

The scattering law has been measured for a powdered beryllium sample at room temperature for energy transfers up to and including $\epsilon=4.0$ ($\hbar\omega=0.1027$ eV). Observed structure in the scattering law data shows that the interference condition for neutron-phonon interactions in coherent scatterers manifests itself in the details of the scattering from even a polycrystal sample, and that the structure is most pronounced at low frequencies (low-energy transfers) where the conditions for scattering are most restrictive. It would appear from this experiment that the incoherent approximation is inadequate for describing the details in the scattering data. The first moment of the energy transfer with respect to the scattering law has been evaluated for these data and found to be high at low-momentum transfers. This discrepancy is attributed to multiple scattering in the sample.

ACKNOWLEDGMENTS

The author is indebted to Dr. R. M. Brugger and Dr. P. D. Randolph for helpful discussions regarding the interpretation of the results of the experiment, to Miss B. K. Sidle for handling the data reduction and programming the averaging procedure, and to Dr. R. G. Fluharty for continued support.

PHYSICAL REVIEW VOLUME 136, NUMBER 5A 30 NOVEMBER 1964

Hyperfine Structure of V_k Centers in Alkali Fluoride Crystals*†

C. EDWARD BAILEY
Department of Physics, Dartmouth College, Hanover, New Hampshire
(Received 2 July 1964)

V_k centers in LiF, NaF, KF, RbF, and CsF are studied. It is shown that the V_k center is stable in all the alkali fluorides at liquid-nitrogen temperature and unstable at room temperature. The results for LiF are in excellent agreement with earlier results. The predictions of the theoretical Hamiltonian derived by Castner, Woodruff, and Känzig are in excellent agreement with all of the experimental results. Values of $g_{\parallel}$, $g_{\perp}$, a, and b are presented for NaF and KF. It is shown that the linewidths of the V_k spectrum depend rather heavily on the nearest-neighbor atoms (the alkalis), and the relaxation process seems to be one of hyperfine coupling.

I. INTRODUCTION

MANY different color centers have been studied in the alkali halides.[1] We will treat the V_k center in the alkali fluorides in some detail. This center has been studied in great detail by Castner, Woodruff, and Känzig.[2–4] The electron paramagnetic resonance (EPR) data have shown that this center is a hole shared between two negative halide ions in the crystal or, in other words, can be thought of as the molecular-ion X_2^-. Optical studies are in agreement with this model.[5–7] Gassinelli and Mieher, using electron-nuclear double-resonance (ENDOR) techniques on LiF, show that their data can be explained by this model.[8,9] From this model it is seen that the centers can lie along each of the six equivalent ⟨110⟩ directions and in the absence of strain or other anisotropic conditions will populate these sites with equal abundance.

The EPR spectrum that one observes for this center results from a very large electron-nuclear interaction, giving rise to a well-resolved hfs. Because this is a hole center, the wave function of the unpaired hole may be

* This work was supported by a grant from the National Science Foundation.

† Based on a thesis submitted to the faculty of Dartmouth College in partial fulfillment of the requirements for the M.A. degree.

[1] See, for example, F. Seitz, Rev. Mod. Phys. **26**, 7 (1956); or J. H. Schulman and W. D. Compton, *Color Centers in Solids* (Pergamon Press, Inc., New York, 1963).

[2] W. Känzig, Phys. Rev. **99**, 1890 (1955).

[3] T. G. Castner and W. Känzig, Phys. Chem. Solids **3**, 178 (1957).

[4] T. O. Woodruff and W. Känzig, Phys. Chem. Solids **5**, 268 (1958).

[5] C. J. Delbecq, B. Smaller, and P. H. Yuster, Phys. Rev. **111**, 1235 (1958).

[6] C. J. Delbecq, W. Hayes, and P. H. Yuster, Phys. Rev. **121**, 1043 (1961).

[7] W. Hayes and G. M. Nichols, Phys. Rev. **117**, 993 (1960).

[8] R. Mieher and R. Gazzinelli, Bull. Am. Phys. Soc. **9**, 88 (1964).

[9] R. Gazzinelli and R. Mieher, Phys. Rev. Letters **12**, 644 (1964).